ARTICLE OPEN

Check for updates

Wireless electromagnetic neural stimulation patch with anisotropic guidance

Bjarke Nørrehvedde Jensen[1], Yuting Wang[1,2], Alice Le Friec[1], Sadegh Nabavi[3,4,5], Mingdong Dong[6], Dror Seliktar[7] and Menglin Chen[1,6]✉

The human body is limited in healing neurological damage caused by diseases or traumatic injuries. Bioelectricity is a quintessential characteristic of neural tissue and has a crucial role in physiological and neurological therapeutics development. Here, a wireless electromagnetic neural stimulation patch was created, combining stimulation through electromagnetic induction with physical guidance cues through structural anisotropy. The melt electrowritten biocompatible, bioresorbable polycaprolactone anisotropic structure with glancing angle deposition of 80 nm gold directly endowed incorporation of a wireless energy harvesting component in the patch, as an electromagnetic stimulation delivery system directly interfacing with neural cells. The biocompatibility and the capacity of the patch to deliver electromagnetic stimulation and promote neurite outgrowth was confirmed in vitro. Electromagnetically (60 mV, 40 kHz, 2 h/day, 5 days) stimulated PC12 cells showed 73.2% increased neurite outgrowth compared to PC12 cells grown without electromagnetic stimulation. The neural stimulation patch shows great potential for wireless electromagnetic stimulation for non-invasive neurological therapeutics advancement.

npj Flexible Electronics (2023)7:34 ; https://doi.org/10.1038/s41528-023-00270-3

INTRODUCTION

The electrophysiological properties of cells and their surrounding tissue in general underlie many functions in living organisms[1]. Electrical stimulation is known to influence numerous biological processes such as angiogenesis, cell division, cell signaling, and nerve sprouting[2]. More importantly, electrical stimulation has been found to enhance functional recovery after nerve injury or surgical repair and promote the speed and accuracy of motor axonal regeneration[3,4].

Electroactive materials have been used in neural tissue to interface with neurons and promote tissue regeneration. Electrical stimulation can be delivered through conductive materials such as polypyrrole, polyaniline, and gold which then induce electrophysiological changes at the cell membrane[5,6]. Especially, a characteristic of gold in biomedical applications is its biocompatibility and low cytotoxicity, making it highly suitable for in vitro and in vivo applications. Gold causes minimal inflammation or allergic reactions, and has been proven to be safe when in contact with organs (such as skin) and tissues (such as oral mucosa)[7,8]. Electrical stimulation can affect membrane proteins by altering surface charge densities, ultimately influencing enzyme activities, ion channels, and membrane receptor complexes. These changes result in cellular uptake of calcium through activating calcium ion channels such as the L-VGCC and TRPC1 channels[6,9]. Calcium functions in neural cells as a signaling agent, regulating gene expression on a transcriptional level and eventually growth-related processes[9,10]. Furthermore, cytoplasmic calcium has been identified as a trigger for growth cones to respond to guidance factors and to regulate the rate of growth cone extension[11].

Delivery of electrical stimulation requires cumbersome external wiring unless a wireless power transfer system is incorporated into the stimulation system. Electromagnetic (EM) induction works by generating electrical current in a receiver coil upon exposure to a changing magnetic field. EM induction has been successfully used by Choi et al. to create a fully implantable and bioresorbable cardiac pacemaker. This poly(lactic-co-glycolic acid) (PLGA) encapsulated wolfram-coated magnesium coil was biocompatible and could effectively transfer power at a distance of up to 15 cm through native tissue. The cardiac coil showed promise in treating transient atrioventricular nodal heart block in mouse models[12]. The same coil design was connected through PLGA-encapsulated magnesium wires to two electrodes held in place by a PLGA nerve cuff for transient electrical stimulation of the sciatic nerve. Wireless electrical stimulation (monophasic, 200 µs pulse, 20 Hz frequency) was delivered to an injured nerve for 1 h per day for 1-, 3-, and 6-days post injury. The results showed significantly increased rates and degrees of nerve regeneration in addition to increased recovery of muscle function[13]. Han et al. developed a wireless EM stimulation system for direct interfacing with cells by growing a flat circular graphene ring using chemical vapor deposition. Despite requiring high frequencies (25 kHz) to create biologically relevant currents, enhanced neuronal differentiation, formation of neurites, and viable neural stem cells were observed[14]. However, while these systems could directly interact with the target tissue, they lacked critical topographical cues found in neural tissue.

Scaffold surface morphology greatly influences neural growth[15]. In a nervous system, neuroglial cells provide a supportive environment in neural tissue for neural outgrowth during development and regeneration. These neuroglial cells (astrocytes, microglia, and oligodendrocytes in the central nervous system and

[1]Department of Biological and Chemical Engineering, Aarhus University, Aarhus, Denmark. [2]School of Mathematics and Physics, University of Science and Technology Beijing, 100083 Beijing, China. [3]DANDRITE, The Danish Research Institute of Translational Neuroscience, Aarhus University, Aarhus, Denmark. [4]Center for Proteins in Memory – PROMEMO, Danish National Research Foundation, Aarhus University, Aarhus, Denmark. [5]Department of Molecular Biology and Genetics, Aarhus University, Aarhus, Denmark. [6]Interdisciplinary Nanoscience Center, Aarhus University, Aarhus, Denmark. [7]Faculty of Biomedical Engineering, Technion – Israel Institute of Technology, Haifa 32000, Israel. ✉email: Menglin@BCE.au.dk

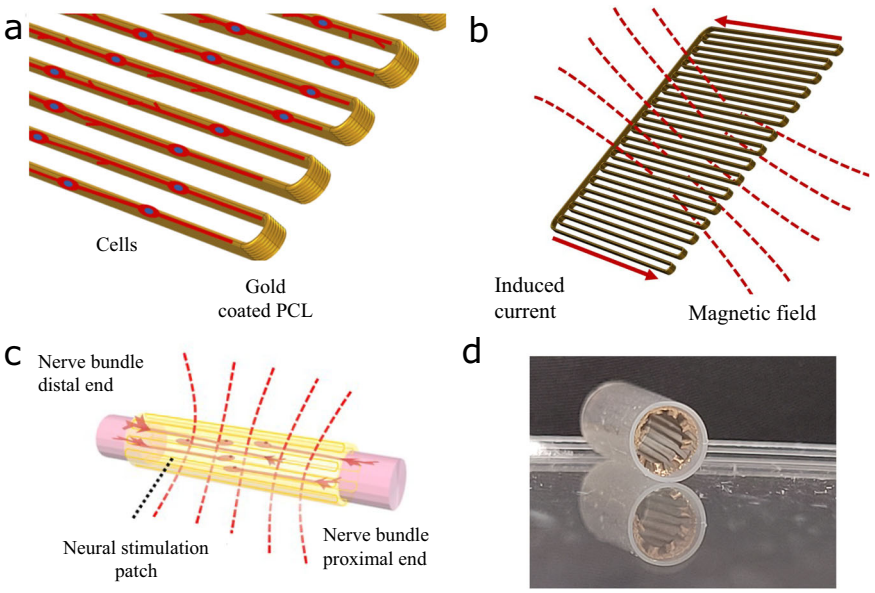

Fig. 1 Schematic illustration of wireless neural stimulation patch. a Close-up of structure illustrating the anisotropic features of the structure with neural cells growing along the structure. **b** Structure overview of the EM neural patch. **c** Application of the patch in delivering stimulation directly to the target nerve bundle. **d** Photograph of neural stimulation patch in plastic tubing with a diameter of 3.2 mm.

Schwann cells in the peripheral nervous system) guide neural outgrowth through release of neurotrophic factors and by synthesizing the extracellular matrix (ECM) with surface ligands, oriented shape, and structural organization[15]. Nano and micro-grooves on the surface of nano/micro fibers are utilized in neural tissue engineering to align neurons and mimic ECM structures that occur in mature nervous systems[16,17]. These anisotropic structural features can function as cues for guiding growth[18,19]. Anisotropic cues can also be created by aligned fibers which can be fabricated by melt electrowriting (MEW), a high-resolution additive manufacturing technique capable of producing fibers in the micro- and nanometer range. This has for example been utilized to create anisotropic architectures for bioactive nerve guidance[20] and guided myogenesis[21,22]. The anisotropic cues must be designed with dimensions that support the intended cue. Based on the structure dimensions (width, height, thickness, orientation, spacing), growth effects such as neurite bridging[23], perpendicular or parallel growth[24], and growth along grooves or ridges[25] have been observed.

Here, a wireless anisotropic EM stimulation patch was created to combine electrical stimulation through EM induction with physical guiding cues through structural anisotropy (Fig. 1). The MEW printed anisotropic structure of biocompatible, biodegradable polycaprolactone (PCL) with glancing angle deposition (GLAD)-mediated 80 nm gold coating directly employed the energy harvesting component (induction coil) as the stimulation delivery interface that the cells (Fig. 1a, b) are in direct contact with. Although PLGA shows great biocompatibility, its high melting temperature hindered its processability to be inferior compared to PCL. In order to design flexible substrate materials with groove patterned structures to guide neural outgrowth, PCL was selected in this work[26]. The patch was structurally and chemically characterized, while its biocompatibility and electromagnetic stimulation effect on a neuron model cell line, PC12 cells, was characterized by means of immunochemistry. It is foreseen that the flexible neural stimulation patch can wrap around the damaged nerve bundle (Fig. 1c, d), interfacing directly with the diseased tissue for delivery of EM stimulation and guided regeneration.

RESULTS AND DISCUSSIONS

Circular neural stimulation patch

The wireless electrical stimulation was first attempted using the classic circular EM coil design (Fig. 2a). The structure was fabricated using MEW to create biocompatible, PCL fibers with a diameter of 10 µm (Fig. 2b). The fibers were printed in a spiral with 400 µm spacing, 15 turns continuously to create a 30-layer stack (Fig. 2c) of a circular structure with a radius of 0.68 mm. The patch was rendered conductive through coating with 50 nm of gold using sputtering and the induction efficiency upon application of an alternating magnetic field was demonstrated using the measured voltage output under known input voltage (Fig. 2d–f). Voltages in the range of 10 mV to 60 mV can be induced by transmitters voltages from 2 V to 6 V at frequencies of 10 kHz to 100 kHz. Although the wireless electrical stimulation (20 mV, 10 kHz) induced longer neurites during the PC12 differentiation (Fig. 2n), as shown in the immunocytochemical staining (Fig. 2g–l), the neurite length was found much shorter in the center with a larger curvature (Fig. 2m) than those at the edge. It is intriguing to see the neurite length (Fig. 2n) increases along with the increased arc length at decreased curvature but limited to the arc length (Fig. 2m). It is well known that cell orientation can be affected by the topographic nature of the substrate, a phenomenon referred to as “contact guidance”. Tresco et al. conducted a quantification of neurite outgrowth direction that demonstrated a strong bias in the direction of minimum curvature that could be explained mechanically as a function of nerve process bending stiffness. A bundle of up to 40 microtubules show a bending stiffness of 2.2E-23 Nm for each tubule and a bundle length on the order of microns[27]. These findings are consistent with observations of microtubule structure in the central and peripheral domains of the growth cone of neurites, suggesting that the mechanical properties of cytoskeletal microtubules may play a regulatory role in determining the outgrowth trajectory[27,28].

Anisotropic neural stimulation patch

Therefore, in order to enhance neurite outgrowth, we designed a neural stimulation patch removing the curvature factor. The principle of the neural stimulation patch is illustrated in Fig. 2,

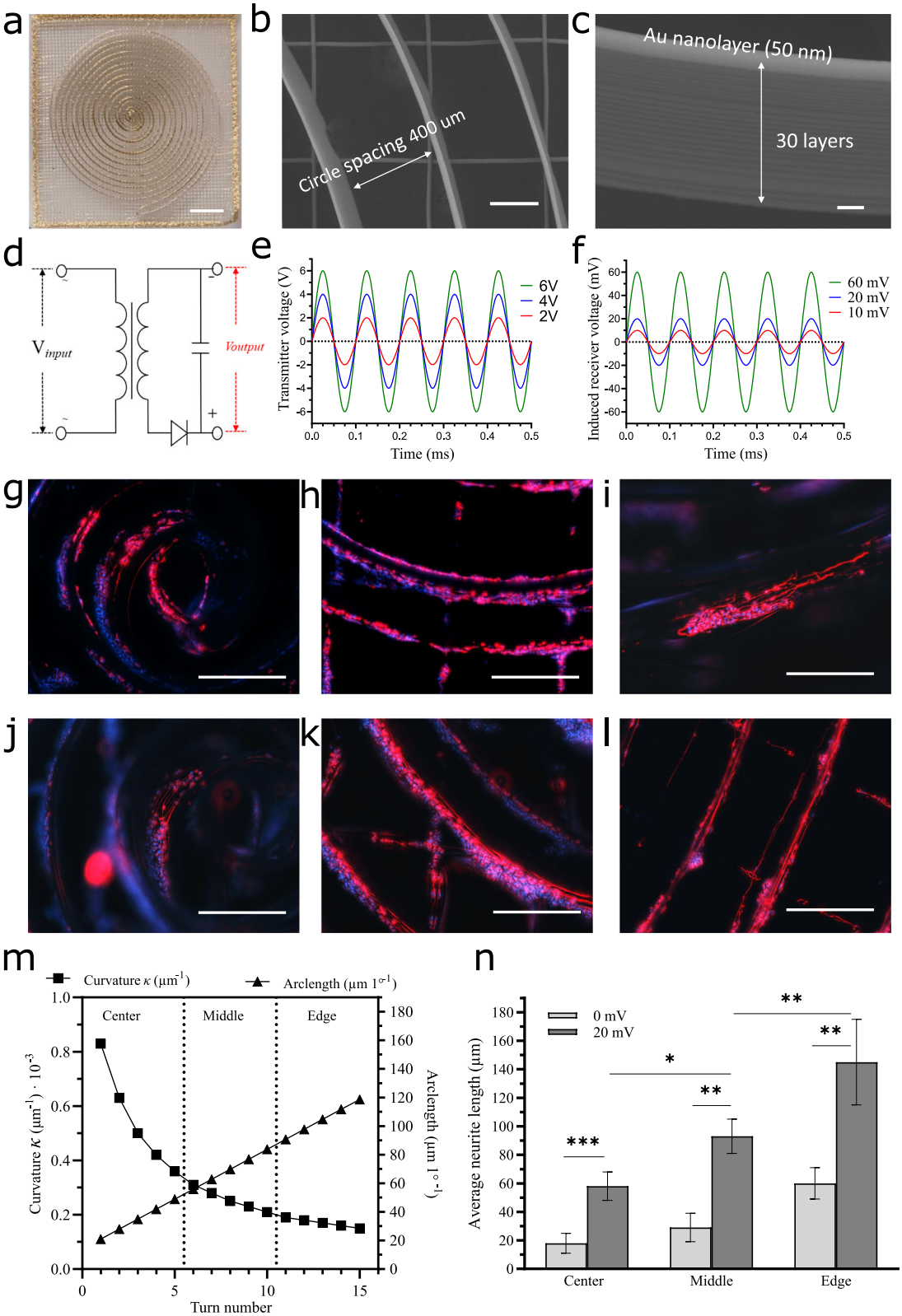

Fig. 2 EM stimulation of PC12 cells on a circular neural stimulation patch. Photograph, scale bar: 2.5 mm (**a**), SEM top view, scale bar: 200 μm (**b**) and SEM side view, scale bar: 20 μm (**c**) of circular neural stimulation patch. **d** Circuit schematic of transmitter coil and neural stimulation patch. **e** Voltage input in transmitter coil and corresponding voltage output (**f**) in the circular neural stimulation patch. Fluorescence images of PC12 cells at the center (**g**, **j**), middle (**h**, **k**) and edge (**i**, **l**) of the circular stimulation patch post 5 days of differentiation with 20 mV, 10 kHz stimulation for 2 h/day. (Red: β-III-tubulin. Blue: Hoechsts. Scale bars, 400 μm). **m** Theoretical curvature κ and arclength $1^{\circ\,-1}$ of the theoretical circumference of each turn of the circular neural stimulation patch starting from the center going outwards. **n** Quantified average neurite length on circular stimulation patch post 5 days of differentiation with 20 mV, 10 kHz stimulation for 2 h/day. Statistical data between the corresponding groups are denoted as $^{*}p < 0.05$, $^{**}p < 0.01$ and $^{***}p < 0.001$. Error bars: standard deviation.

which shows a thin, flexible, melt electrowritten stimulation patch with anisotropic cues for wireless stimulation of nerve tissue. The structure was fabricated again using MEW creating fibers 15 µm in diameter of PCL in a 15-layer stack of fibers that resembles a grooved wall. The grooves function as anisotropic cues to guide the cells in direct contact to extend their neurites (Fig. 1a). The patch was rendered conductive through coating with 80 nm of gold using GLAD. The closed loop configuration enables induction of current in the patch upon application of an alternating magnetic field as illustrated in Fig. 1b. The current is used for electrically stimulating cells in contact with the neural stimulation patch further supporting growth of neural tissue. The intended use is for interfacing with damaged nerve bundles as illustrated in Fig. 1c. The anisotropic features of the wall are placed along the bundle thus functioning as topographical guidance cues. The neural stimulation patch can wrap around the nerve bundle due to its flexibility as demonstrated in Fig. 1d. The patches can be customized to cover more area by adding multiple patches in conjunction, or by fabricating a larger stimulation patch.

SEM images in Fig. 3 show the walls of the patch and their anisotropic features. The gold-coated patch (Fig. 3a) has an isotropic support grid beneath (1 cm by 1 cm with 250 µm wall spacing), and the coil structure is 7.75 mm by 8.25 mm with 250 µm wall spacing. The support structure is visible underneath the walls in Fig. 3ab, which are keeping the walls in place. The grooved features are visible in Fig. 3c which are created by the layer-by-layer deposition of the fiber during the MEW process.

GLAD is a physical vapor deposition process where the deposition flux is incident at a large angle with respect to the surface normal and the substrate is rotating. GLAD produces a gradient through the effect of shadowing during the deposition. EDX mapping of GLAD gold coating shows the distribution of gold over the side of the wall (Fig. 3e). Further analysis of the relative element quantity (Fig. 3f) confirmed the gradient of gold coating with 2.59% Au at the lowest part of the wall and 5.73% Au at the highest part of the wall. The gold is mainly situated at the top of the wall limiting conductance between the wall and the supporting grid, which is crucial for efficient EM induction. The gold coating was further distributed down the side of the wall when sputter deposition (Supplementary Fig. 1) was used instead of GLAD. However, it was found that this caused connections between the wall and the support structure and lowered induced voltage. All in all, the results show the successful fabrication and GLAD gold coating of the neural stimulation patch.

The next step was to analyze the voltage output induced in the neural stimulation patch upon application of an alternating magnetic field. The voltage induced in the patch in such a setup as shown in Fig. 3g–i, voltages in the range of 10 mV to 140 mV can be induced by transmitters voltages from 5 V to 10 V at frequencies of 10 kHz to 100 kHz. Similar parameters (25 kHz) have been used by Han et al. who demonstrated enhanced neural growth in neural stem cells from mice[14].

Biocompatibility

The biocompatibility of the patch and electromagnetic stimulation was investigated through LDH, a cytotoxicity assay, and live/dead imaging. After 24 h of PC12 cells culturing on PCL patches (group PCL), and gold-coated patches (group PCL-Au) with stimulation for 2 h with 60 mV at 40 kHz (group EM), the cytotoxicity was measured by LDH assay (Supplementary Fig. 2a). No significant changes of cytotoxicity compared to TCP (low control, 0%) was observed, indicating that the neural stimulation patch and the EM stimulation are biocompatible with PC12 cells. This is further supported by the results of live/dead imaging shown in Supplementary Fig. 2b–d, where few to no dead cells (red indicated with white arrows) were found in the fluorescence images.

Effect of electromagnetic stimulation on neural differentiation

The neurite growth enhancing effect of the electromagnetic stimulation delivered by the patch was investigated by the use of immunochemistry staining of the β-III-tubulin as a cytoskeletal neural marker. Figure 4a, b shows fluorescence images of cells grown on the patch without EM stimulation (a) and with 5 days (2 h/day) EM stimulation (b), respectively. Clusters of cells with EM stimulation are more visible, indicating a higher presence of β-III-tubulin and neurite outgrowth. This is further supported by neurite tracing results (Fig. 4c). EM stimulation significantly increased neurite outgrowth of PC12 cells at 3-days, 5-days, and 7-days of EM stimulation (2 h/day, 60 mV, 40 kHz) when grown on the stimulation patch. The mean neurite lengths were 89.50 ± 42.01 µm, 106.59 ± 58.79 µm, and 178.45 ± 63.56 µm at 3-days, 5-days, and 7-days without EM stimulation, respectively; and 131.62 ± 59.38 µm, 184.57 ± 81.42 µm, and 271.58 ± 109.97 µm at 3-days, 5-days, and 7-days with EM stimulation (2 h/day, 60 mV, 40 kHz), respectively. The EM stimulation thus significantly increased neurite outgrowth by 47%, 73%, and 52% at 3 days, 5 days, and 7 days of stimulation, respectively. The magnetic field used for inducing a 60 mV at 40 kHz had no significant neural growth enhancing effect on a similar scaffold design without the gold coating required to induce currents (Supplementary Fig. 3). The results show that a sustained, significant increase in neurite outgrowth can be achieved through wireless EM stimulation on the neural stimulation patch. A representative confocal fluorescence image of PC12 cells after 7 days of EM stimulation on the patch is shown in Fig. 4d. Neurites of several hundreds of micrometers in length were observed growing in the grooves on the side of the wall. The results show improved neurite outgrowth compared to similar direct stimulation devices such as the silver nanowire electrodes reported by Xu et al. that yielded average neurite lengths of 140.48 ± 30.15 µm after 5 days of electrical stimulation (60 mV, 20 Hz, 4 h/day)[29]. Furthermore, comparing neurite outgrowth on the circular neural stimulation patch (Fig. 2n) with the neurite outgrowth of the straight neural stimulation patch (Fig. 4c) an increase from ~60 µm to ~106 µm at 5 days without stimulation is observed. This further supports Tresco et al.'s findings on the influence of substrate curvature on the outgrowth of neurites[27,28]. Furthermore, we compared the performance of our device with other literatures to demonstrate improvements in wireless systems in Table 1. This indicates that our device not only exhibits wireless advantages, making the electrical stimulation process more convenient, but also shows significant improvements under the synergetic effects of structural guidance and EM stimulation.

The high frequency (40 kHz) required for inducing a 60-mV potential in the neural stimulation patch is outside the commonly used frequency range of 1–500 Hz[30]. However, study of Han et al. has also shown that high-frequency stimulation (25 kHz) can induce neural outgrowth[14]. A review[30] on of kilohertz-frequency stimulation on the nervous system (both in vitro and in vivo) concludes that despite a growing interest and clinical applications in kilohertz-frequency stimulation and neural modulation, the underlying mechanisms are still poorly understood, which calls for further research. Furthermore, it is possible to convert the kilohertz-frequency stimulation to low-frequency DC-like currents by incorporating radiofrequency positive-intrinsic-negative (PIN) diodes. In the work by Choi et al. a bioresorbable PIN diode based on a doped monocrystalline silicon nanomembrane was developed and incorporated into a bioresorbable, battery-free cardiac pacemaker. The PIN structured diode in reverse bias with a long reverse-recovery time functions as a parasitic capacitor at high frequencies (>1 MHz), creating a rippled DC-like current[12]. Future versions of the neural stimulation patch design can thus benefit from incorporating a radiofrequency PIN diode, mitigating the high-frequency reliance of the current design.

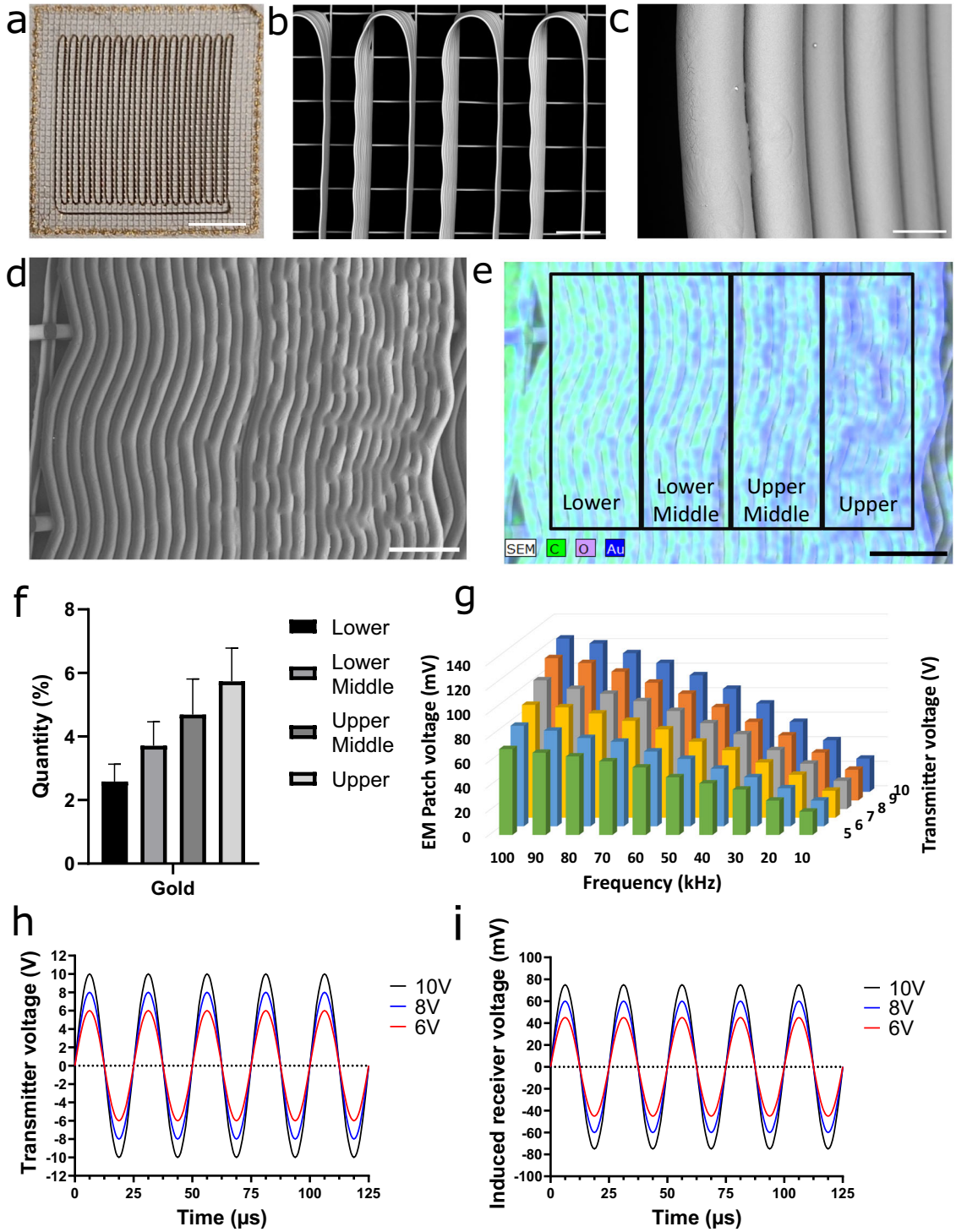

Fig. 3 SEM, EDX analysis and EM induction analysis of gold coated neural stimulation patch. a Photograph of gold coated neural stimulation patch. Scale bar: 2500 µm. **b**–**d** SEM image of gold coated neural stimulation patch at different magnifications. Scale bars, **b**: 250 µm, **c**: 10 µm, **d**: 100 µm. **e** EDX mapping of **d** with four zones used for quantitative analysis of surface coating (**f**), scale bar: 100 µm. ($n = 8$). **g** 3D plot of the voltage induced in the neural stimulation patch ($n = 4$). Waveform and voltage magnitude in transmitter coil (**h**) and the resulting induced voltage in neural stimulation patch (**i**) ($n = 4$). Error bars: standard deviation.

Electrophysiology of electromagnetically stimulated cells

Whole-cell electrophysiology measurements were performed to investigate the effect of EM stimulation on the excitability of PC12 grown on the neural stimulation patch (Fig. 5). Current measurements on differentiated PC12 cells on neural stimulation patch (Fig. 5d) were performed and normalized to cell size through cell capacitance. No significant difference (Fig. 5c) in cell excitability between PC12 grown on neural stimulation patches without (Fig. 5a) and with EM stimulation (Fig. 5b) was found. Inducing neurite outgrowth from PC12 cells using NGF has long been

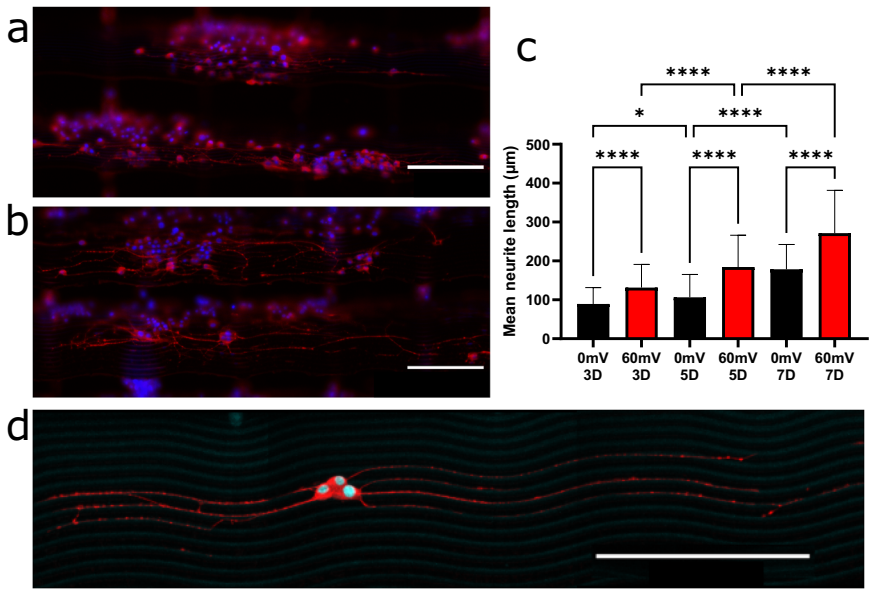

Fig. 4 Effect of neural stimulation patch on neurite growth of PC12 cells. Representative fluorescence images of PC12 cells grown on neural stimulation patch for 5 days either without (**a**) or with (**b**) EM stimulation. Cell nucleus stained blue and cytoskeletal β-III-tubulin stained red. **c** Neurite length quantification of PC12 cells grown on neural stimulation patch with and without EM stimulation for 3 days, 5 days, and 7 days ($n > 300$). Statistical analysis performed using one-way Kruskal–Wallis test with Dunn's multiple comparisons test. **d** Confocal image of PC12 cells on neural stimulation patch after 7 days of EM stimulation (60 mV, 40 kHz, 2 h/day, 7 days). Scale bars: 200 μm. Statistical data between the corresponding groups are denoted as $*p < 0.05$, $**p < 0.01$, $***p < 0.001$ and $****p < 0.0001$. Error bars: standard deviation.

Table 1. Comparison of the performance of PC12 nerve cells grown on different devices under electric stimulation.

Materials	Best performance (neurite length/μm)	Differentiation under electric stimulation	Wired/wireless	Refs.
PEDOT:PS wrinkled polymer	90.9 ± 4.8 μm	5 days	Wired	[18]
Polypyrrole onto parallel-aligned poly(L-lactide) fibers	~32.05 μm	3 days	Wired	[40]
Graphene-biopolymer	~75 μm	3 days	Wired	[41]
Conductive MEH-PPV:PCL electrospun nanofibres	97 ± 24 μm	7 days	Wired	[42]
Gold Nanoparticles	~100 μm	3 rounds	Wired	[43]
Au-PCL scaffold	~100.5, and 11.4–200.5 μm	5, 10, and 20 days	Wired	[8]
Neural stimulation patch	131.62 ± 59.38 μm, 184.57 ± 81.42 μm, and 271.58 ± 109.97 μm	3, 5, and 7 days	Wireless	This work

known to induce ion channel formation and cell excitability in PC12 cell[15,31–33]. Electrical stimulation has likewise been found to induce pathways involved in neurite outgrowth[9]. Thus, electrical stimulation could be postulated to likewise increase the excitability of PC12 cells. However, the results in Fig. 5 show that when accounting for the size of the cell through cell capacitance, the cell excitability remains similar with and without electrical stimulation during NGF-induced PC12 differentiation. This indicates that electrical stimulation induces increased cell size without altering the density of excitability.

Towards nerve guide conduit

The flexibility of the neural stimulation patch is a crucial aspect for its functionality as a nerve guide conduit. It is essential that the patch maintains its conductivity and inductive capabilities when it is rolled into a tubular structure. To demonstrate its flexibility, the neural stimulation patch was rolled into a silicone tube with a diameter of 3.2 mm (Fig. 6a). The results indicate that the neural stimulation patch is sufficiently flexible to accommodate the diameter of larger human peripheral nerves[34,35].

SEM images of the rolled neural stimulation patch (Fig. 6c–e) revealed no signs of cracks in the gold coating, supporting that the inductive function of the neural stimulation patch should be retained even when rolled. This is similar to the results of our earlier work that demonstrated the stability of the gold coting and conductivity of highly flexible 80 nm gold-coated PCL grid scaffolds upon bending and repeat injections[8].

Mechanical measurements of the stress-strain curve (Fig. 6g) demonstrated minor variations in the tensile stress behavior in both the longitudinal and perpendicular directions relative to the wire orientation. However, ~3.5 fold more force was needed to yield the same strain for the longitudinal direction caused by the longitudinal anisotropic features of the neural stimulation patch (Supplementary Fig. 4a). No significant difference in Young's modulus between the longitudinal direction (304.46 ± 11.24 MPa) and the perpendicular direction (320.83 ± 92.07 MPa) (Supplementary Fig. 4b) was observed, aligning with previous findings of the Young's modulus of PCL[36,37].

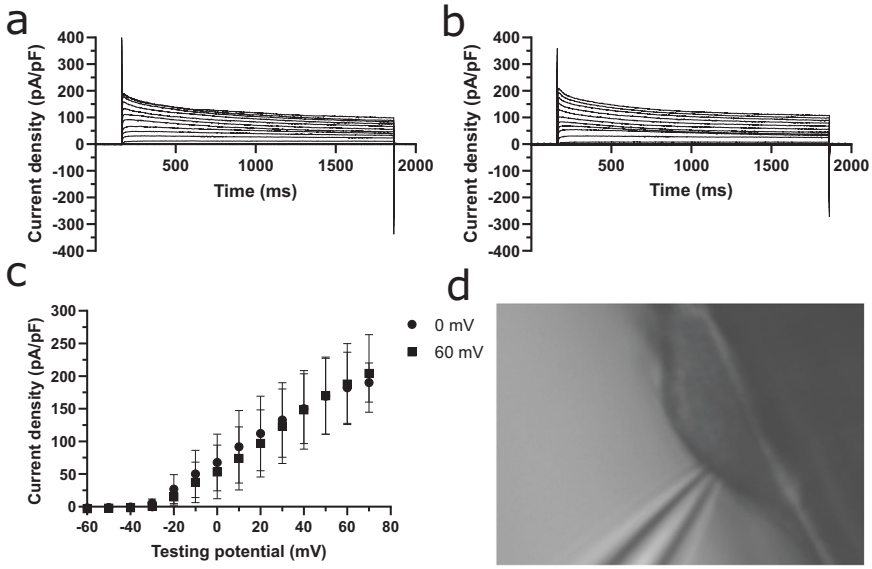

Fig. 5 Electrophysiology recordings of PC12 cells differentiation on neural stimulation patches for 7 days with/without 60 mV at 40 kHz stimulation for 2 h/day. a Average current density traces of PC12 cells without stimulation during differentiation ($n = 6$). **b** Average current density traces of PC12 cells with EM stimulation during differentiation ($n = 6$). **c** Comparison of current densities of PC12 cells with and without EM stimulation during differentiation. **d** Photo of differentiated PC12 cell situated on side of neural stimulation patch wire during whole-cell electrophysiology recording. Error bars: standard error.

To assess the EM inductive function of the neural stimulation patch when rolled, it was exposed to an alternating magnetic field of a similar magnitude as in previous experiments (Fig. 3g). The induced voltage was measured and compared (Supplementary Fig. 5). The results showed a reduction in induced voltage from 78 mV (at 100 kHz when flat, Supplementary Fig. 5b) to 68 mV (at 100 kHz when rolled). It is noteworthy that the rolled neural stimulation patch was tested using a 500 µm wire spacing compared to the 250 µm wire spacing used in Fig. 3. As shown in the optimization study, such an increase of the wire spacing caused a major decrease in inductive power (Supplementary Fig. 5a).

However, the induced voltage range used for stimulating PC12 cells in Fig. 4 still falls within the induced voltage range once rolled. This is supported by the fluorescence images of PC12 cells grown and differentiated on neural stimulation patches rolled in silicone tubes with 5 days of EM stimulation at 60 mV, 90 kHz, 2 h/day that show neurite outgrowth with similar trends of growing along the fibers of the neural stimulation patch (Fig. 6h). In summary, the neural stimulation patch retains its inductive function once rolled due to the high flexibility of the PCL scaffold and stability of the gold coating, enabling its potential use as a nerve guide conduit with wireless electrical stimulation and topographical guidance cues.

In summary, a highly flexible MEW printed GLAD gold-coated PCL induction patch was created that enables wireless electromagnetic stimulation of target cells with anisotropic guidance. Gradient gold coating using GLAD rendered the patch conductive and EM transmittable. Voltage outputs in the 10–140 mV range were achieved using 10–100 kHz magnetic fields. Significant increases in neurite outgrowth of PC12 cells upon EM stimulation were observed. The research found that the designed patch can not only promote the neurite outgrowth through wireless electric stimulation, but also further guide the outgrowth by surface microscale anisotropic topography. Due to its good biocompatibility, flexibility, and wireless energy transfer characteristics, the patch holds great potential for the guided repair of damaged nerve tissue by electromagnetic stimulation in the future.

METHODS

Materials and fabrication of the electromagnetic stimulation patch

Polycaprolactone (PCL) was used as raw material and was electrowritten without any modifications (medical grade, PURE-SORB PC 12 PCL, Corbion). Various designs of PCL receiver coil on PCL support grids were electrowritten using a melt electrowriting instrument (CAT000111, Spraybase, Ireland). The structure was designed and written in G-code which was run by a Mach3 motion control software. PCL was melted at 90 °C for 1 h before printing through a stainless-steel needle (24 G). A 10 cm diameter Silicon-wafer was used as a collector at a 4 mm distance from the needle. A 4.75–4.9 kV high voltage was applied between the needle and the collecting plate. A flow rate pressure of 0.85 bar was controlled by a Spraybase® Pressure Driven System. The coil (EM receiver) was printed at a rate of 200–250 mm min^{-1} with a support grid at a rate of 30 mm min^{-1}. The coil structure and support grid were printed with 15 layers and 2 layers, respectively. The G-code used for melt electrowriting of the circular and anisotropic neural stimulation patch can be found in Supplementary Table 1. The resulting patch was subsequently coated with 4 nm titanium and 80 nm of gold using E-beam GLAD (Cryofox Explorer 500 GLAD). During coating the scaffold was tilted 20 degrees and rotated at 3 rpm.

The wireless EM stimulation system used for stimulating neural cell growth is comprised of a receiver coil patch placed in a 24-well plate and a rectangular transmitter coil placed around the well plate. The transmitter coil size is matched to fit around a standard well plate to minimize the distance between the patch and the transmitter coil. The transmitter coil was made of 60 turns of copper wire (11 cm × 15 cm) connected to a Waveform Generator (HP 33120A, Hewlett Packard) supplying alternating current. The voltage and frequency applied through the transmitter coil were adjusted to produce the desired voltage output in the receiver coil scaffold.

Characterization

The resistance of the neural stimulation patch was measured by a semiconductor analyzer (4200 system, Cleveland, USA; $n = 3$). The

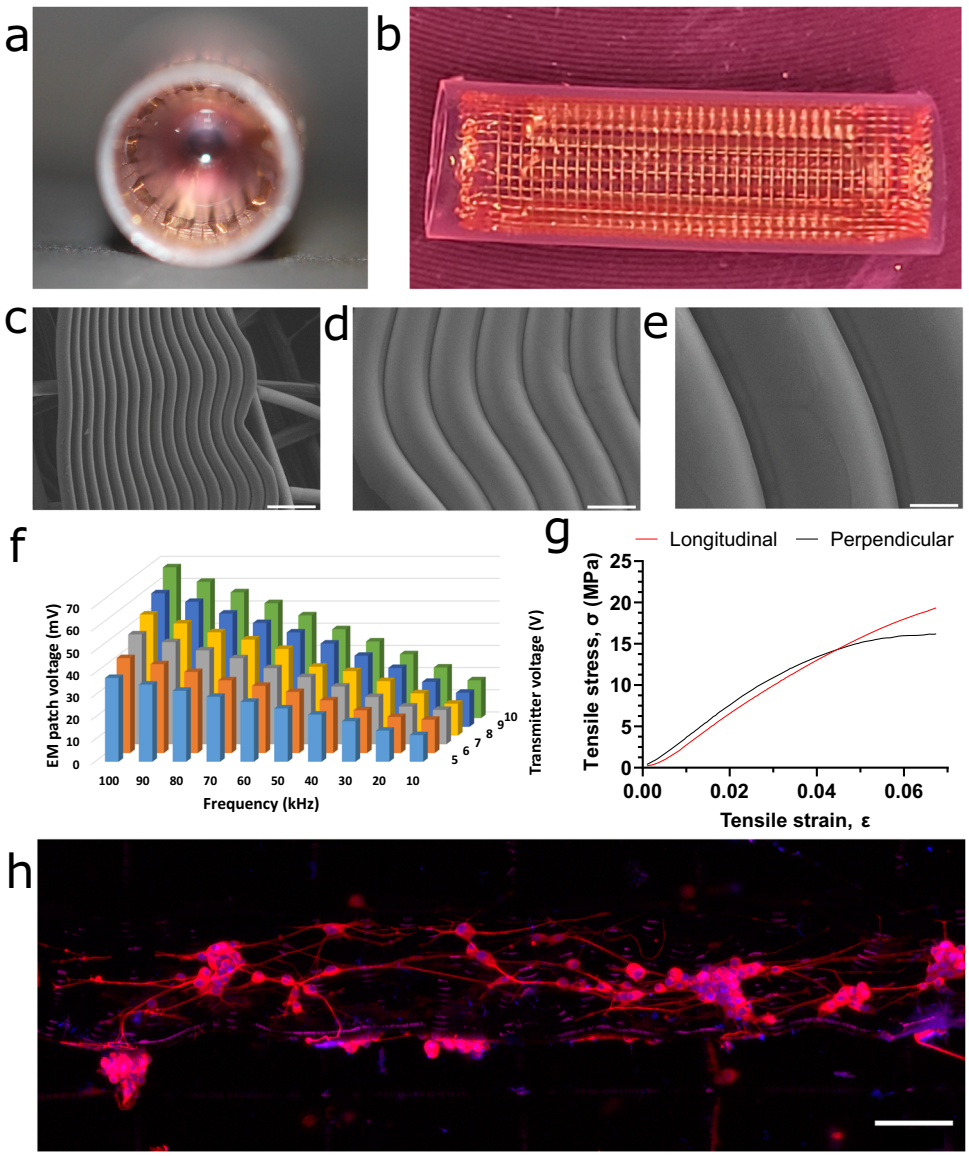

Fig. 6 Scaffold flexibility. a, **b** Photograph of neural stimulation patch rolled into silicone tube (*Diameter* = 3.2 mm) demonstrating the flexibility of the EM patch. **c**–**e** SEM images of neural stimulation patch folded showing surface gold coating integrity. Scale bars, **c**: 100 µm, **d**: 20 µm, **e**: 10 µm. **f** Voltage output of neural stimulation patch ($n = 3$) (500 µm wire spacing) when rolled into silicone tube show in **a** upon excitation with alternating magnetic field (transmitter coil: 11 cm × 15 cm, 60 turns, copper). **g** Stress-strain curve of EM patch showing tension forces longitudinal and perpendicular to wire direction ($n = 3$). **h** Fluorescence image of PC12 cells grown and differentiated on neural stimulation patch rolled into silicone tube after 5 days of differentiation with EM stimulation (60 mV, 90 kHz, 2 h/day, 5 days). Blue = DAPI, red = β-III-tubulin. Scalebar: 100 µm.

voltage output of the receiver coil was recorded by an Agilent DSOX3012A oscilloscope. The morphology and gold coating of the receiver coil patches were evaluated by scanning electron microscopy equipped with an energy-dispersive X-ray spectrometer (SEM, Hitachi, TM3030). Stress-strain curves were measured using a Discovery HR20 rheometer with mechanical clamps. Gold-coated neural stimulation patches were clamped by 2 mm on each side leaving a measurement gap of 6 mm. Tensile stress measurements were performed at a rate of 3 µm/second. Tensile stress and strain were normalized to neural stimulation patch cross-section area.

Cell culture

PC12 cells were cultured directly onto the patch to evaluate the effect of electromagnetic induction on neural cells. PC12 cells were prepared and cultured similarly to previous work[8,20]. A collagen IV coated flask was used to preculture PC12 cells (ATCC® CRL-1721™) in growth medium (15% horse serum (HS), 2.5% fetal bovine serum (FBS), 1% penicillin-streptomycin (P/S) and 0.5% HEPES buffer in DMEM/F12 Glutamax). All patches were UV sterilized (254 nm) for 2 × 30 min in 24-well plates. All patches were coated with collagen IV for 6 h-overnight at 37 °C. Patches not coated with gold were used as controls (group PCL), those coated ones as group Gold and those coated ones that received EM stimulation as group EM. Cell suspensions (100 µL) containing 100 000 PC12 cells were seeded on patches and incubated for 30 min for cell attachment before adding growth medium. The seeded cells were cultured in the growth medium for 1 day and then transferred into wells containing cell differentiation medium (0.5% HS, 0.5% FBS, 1% P/S, and 50 ng ml^{-1} of nerve growth factor

(NGF, 2.5 S, Gibco) in DMEM/F12 Glutamax. First day of stimulation was initiated 1 day after transferring into differentiation media. PC12 cells cultured on the patches were stimulated for 2 h per day throughout the 6-day differentiation period (5 days with stimulation). For clarity, the voltage and frequency are stated in the result section of each experiment. Differentiation media was replenished every second-day post stimulation.

For PC12 cells seeded onto rolled neural stimulation patches the protocol was slightly altered. The neural stimulation patch was first rolled and slid into 1-cm-long silicone rubber tuber (Ø = 3200 µm), UV sterilized for 60 min, and collagen IV coated overnight in 24-well plates. 300 000 PC12 cells were suspended in 80 µL media and injected into each rolled neural stimulation patch silicone tube and incubated for 30 min for cell attachment before adding growth medium. The experiment conditions and timeline were hereafter the same as described above for the flat neural stimulation patch.

Cytotoxicity analysis

Lactate dehydrogenase (LDH) assay was used to analyze the cytotoxicity of the patches. PC12 cells were cultured and maintained as described in the Cell Culture section. Neural stimulation patches were prepared as described in the Materials and Fabrication section. As a low toxicity control, 50,000 PC12 cells were seeded on collagen-coated 24-well tissue culture plate (TCP). As a high toxicity control, 50,000 PC12 cells were grown in 1% Triton X-100 supplemented growth medium. Stimulated groups were stimulated for 2 h (60 mV, 40 kHz, 2 h). After 24 h of culturing the culture media was collected and centrifuged at 1800 RPM for 5 min at 4 °C. The supernatant was subsequently collected and kept on ice in accordance with the manufacture's protocol (Roche Diagnostics, Mannheim, Germany). 50 µL of each replicate ($n = 6$) was loaded into a 96-well plate. 50 µL growth media was loaded as negative control. The reaction mix consisting of a catalyst and dye was mixed at a ratio of 1:45. 50 µL of the reaction mix was added to each sample well and subsequently incubated shielded from light for 30 min at room temperature. After incubation the sample absorbance at 490 nm were measured using a Victor X5 230 Multilabel Reader (PerkinElmer, Waltham, Massachusetts, USA). The percentage cytotoxicity was calculated as follows in Eq. (1):

$$\text{Cytotoxicity}(\%) = \frac{\text{Exp. abs. value} - \text{TCP abs. value}}{\text{Triton abs. value} - \text{TCP abs. value}} \times 100 \quad (1)$$

Live/dead imaging

PC12 cells were cultured and maintained as described in the Cell Culture section. Neural stimulation patches were prepared as described in the Fabrication section. 50,000 PC12 cells were seeded in collagen-coated 24-well TCP plates as control. Patches were moved into new 24-wells after 24 h of culture. After 5 days of culture the sample wells were gently rinsed with warm growth media. Live/dead solution was prepared by diluting Calcein-AM (2 mM in DMSO) 1:1000 and propidium iodide (PI) (1.5 mM in deionized H_2O) 1:500 in 37 °C cell culture medium without serum and phenol red. The growth medium was removed. In all, 300 µL Live/dead solution was added to each sample well and incubated for 30 min at 37 °C and 5% CO_2 protected from light. The live/dead solution was subsequently removed and replaced with cell culture medium without serum or phenol red. Fluorescence imaging was immediately performed using EVOS FL Auto Cell Imaging System (Invitrogen). For Calcein 494 nm/517 nm (excitation/emission) was used and for PI 535 nm/617 nm was used.

Immunostaining and fluorescence imaging

After 6 days of differentiation, samples ($n = 4$ replicates per condition) were fixed in 4% formaldehyde solution for 20 min, and subsequently permeabilized in PBS with 0.2% Triton X-100 for 15 min. After blocking in 1% bovine serum albumin (BSA)/PBS solution for 45 min at room temperature cells were immunostained with mouse anti-βIII-tubulin (Abcam ab78078, 1:1000) primary antibody at 4 °C overnight. After washing with PBS, cells were stained with Donkey anti-mouse (Alexa Fluor 594, Abcam, 1:1000) secondary antibody for 1 h at room temperature. After washing with PBS again, Hoechst 33258 (Life Technologies, 1:10,000) was added for 10 min to stain cell nuclei. Fluorescence images were acquired with an EVOS FL Auto Cell Imaging System (Invitrogen).

Cell neurite length was manually traced and evaluated from cell fluorescence images using ImageJ[38] with NeuronJ[39] plugin-software. Neurites longer than the cell body and not extending outside of the field of view were included. The average neurite length is defined as the total neurite length divided by the total neurite number. At least 300 neurites were measured from each condition. The manual tracing was performed blinded to the experimental condition.

Theoretical curvature and arclength calculations

The radius of the circular neural stimulation patch was calculated from the G-code printing parameters and used for calculating the theoretical curvature, κ, and arclength degree^{-1} using formula (2) and (3), respectively.

$$\kappa = \frac{1}{r} \quad (2)$$

$$\text{Arclength} = 2\pi \cdot r \cdot \frac{1}{360^\circ} \quad (3)$$

Electrophysiology

The electrophysiology of PC12 cells grown on receiver coil patches were recorded in whole-cell current- and voltage-clamp modes. A Multiclamp 700B amplifier (Molecular Devices, Axon Instruments), Digidata 1550A digitizer (Molecular Devices, Axon Instruments), and pClamp 10.7 software (Molecular Devices, Axon instruments) were used for all data acquisition. Borosilicate glass tubes (OD = 2 mm, ID = 1 mm) (Warner Instruments) were pulled into pipettes with a final resistance of 3–5 MΩ using a Model P-1000 micropipette puller (Sutter Instruments). The intracellular solution for all recordings was composed of (in mM): 140 KCl, 2 $MgCl_2$, 10 HEPES, 10 EGTA, 2 Mg-ATP, adjusted to pH 7.3. The extracellular solution was composed of (in mM): 140 mM NaCl, 3 KCl, 1 $MgCl_2$, 2 $CaCl_2$, 10 HEPES, 10 Glucose, adjusted to pH 7.4. Both solutions were pH adjusted using KOH. Measurements were performed at room temperature.

Statistics

The data is represented as a mean ± standard deviation. Statistical significance was analyzed using Kruskal-Wallis test with Dunn's test to correct for multiple comparisons using GraphPad Prism software. The values of $^*p < 0.05$, $^{**}p < 0.01$, $^{***}p < 0.001$, and $^{****}p < 0.0001$ indicates significant difference.

DATA AVAILABILITY

The data that support the findings of this work are available from the corresponding author upon reasonable request.

Received: 15 March 2023; Accepted: 23 July 2023;
Published online: 31 July 2023

REFERENCES

1. Manousiouthakis, E., Park, J., Hardy, J. G., Lee, J. Y. & Schmidt, C. E. Towards the translation of electroconductive organic materials for regeneration of neural tissues. *Acta Biomater.* **139**, 22–42 (2022).
2. Hosoyama, K. et al. Electroconductive materials as biomimetic platforms for tissue regeneration. *Biotechnol. Adv.* **37**, 444–458 (2019).
3. Gordon, T. Electrical stimulation to enhance axon regeneration after peripheral nerve injuries in animal models and humans. *Neurotherapeutics* **13**, 295–310 (2016).
4. Al-Majed, A. A., Brushart, T. M. & Gordon, T. Electrical stimulation accelerates and increases expression of BDNF and trkB mRNA in regenerating rat femoral motoneurons. *Eur. J. Neurosci.* **12**, 4381–4390 (2000).
5. Kiyotake, E. A., Martin, M. D. & Detamore, M. S. Regenerative rehabilitation with conductive biomaterials for spinal cord injury. *Acta Biomater.* **139**, 43–64 (2022).
6. Zhu, R. et al. Electrical stimulation affects neural stem cell fate and function in vitro. *Exp. Neurol.* **319**, 112963 (2019).
7. Zhu, B., Gong, S. & Cheng, W. Softening gold for elastronics. *Chem. Soc. Rev.* **48**, 1668–1711 (2019).
8. Wang, Y. et al. An injectable high-conductive bimaterial scaffold for neural stimulation. *Colloids Surf. B Biointerfaces* **195**, 111210 (2020).
9. Jara, J. S., Agger, S. & Hollis, E. R. Functional electrical stimulation and the modulation of the axon regeneration program. *Front. Cell Dev. Biol.* **8**, 736 (2020).
10. Puri, B. K. *Calcium Signaling* (ed. Islam, Md. S.) 537–545 (Springer International Publishing, 2020).
11. Hong, K., Nishiyama, M., Henley, J., Tessier-Lavigne, M. & Poo, M. Calcium signalling in the guidance of nerve growth by netrin-1. *Nature* **403**, 93–98 (2000).
12. Choi, Y. S. et al. Fully implantable and bioresorbable cardiac pacemakers without leads or batteries. *Nat. Biotechnol.* https://doi.org/10.1038/s41587-021-00948-x (2021).
13. Koo, J. et al. Wireless bioresorbable electronic system enables sustained nonpharmacological neuroregenerative therapy. *Nat. Med.* **24**, 1830–1836 (2018).
14. Han, F. et al. Strategy for designing a cell scaffold to enable wireless electrical stimulation for enhanced neuronal differentiation of stem cells. *Adv. Healthc. Mater.* **10**, 2100027 (2021).
15. Simitzi, C., Ranella, A. & Stratakis, E. Controlling the morphology and outgrowth of nerve and neuroglial cells: the effect of surface topography. *Acta Biomater.* **51**, 21–52 (2017).
16. Hoffman-Kim, D., Mitchel, J. A. & Bellamkonda, R. V. Topography, cell response, and nerve regeneration. *Annu. Rev. Biomed. Eng.* **12**, 203–231 (2010).
17. Hussey, G. S., Dziki, J. L. & Badylak, S. F. Extracellular matrix-based materials for regenerative medicine. *Nat. Rev. Mater.* **3**, 159–173 (2018).
18. A. Bonisoli, A. Marino, G. Ciofani, F. Greco. Topographical and electrical stimulation of neuronal cells through microwrinkled conducting polymer biointerfaces. *Macromol. Biosci.* https://doi.org/10.1002/mabi.201700128 (2017).
19. Gong, H. Y. et al. A novel conductive and micropatterned PEG-based hydrogel enabling the topographical and electrical stimulation of myoblasts. *ACS Appl. Mater. Interfaces* **11**, 47695–47706 (2019).
20. Zhang, Z. et al. 3D anisotropic photocatalytic architectures as bioactive nerve guidance conduits for peripheral neural regeneration. *Biomaterials* **253**, 120108 (2020).
21. Zhang, Y., Le Friec, A. & Chen, M. 3D anisotropic conductive fibers electrically stimulated myogenesis. *Int. J. Pharm.* **606**, 120841 (2021).
22. Zhang, Y., Zhang, Z., Wang, Y., Su, Y. & Chen, M. 3D myotube guidance on hierarchically organized anisotropic and conductive fibers for skeletal muscle tissue engineering. *Mater. Sci. Eng. C* **116**, 111070 (2020).
23. Goldner, J. S., Bruder, J. M., Li, G., Gazzola, D. & Hoffman-Kim, D. Neurite bridging across micropatterned grooves. *Biomaterials* **27**, 460–472 (2006).
24. Gomez, N., Lu, Y., Chen, S. & Schmidt, C. E. Immobilized nerve growth factor and microtopography have distinct effects on polarization versus axon elongation in hippocampal cells in culture. *Biomaterials* **28**, 271–284 (2007).
25. Johansson, F., Carlberg, P., Danielsen, N., Montelius, L. & Kanje, M. Axonal outgrowth on nano-imprinted patterns. *Biomaterials* **27**, 1251–1258 (2006).
26. Behtaj, S., Karamali, F., Masaeli, E., G. Anissimov, Y. & Rybachuk, M. Electrospun PGS/PCL, PLLA/PCL, PLGA/PCL and pure PCL scaffolds for retinal progenitor cell cultivation. *Biochem. Eng. J.* **166**, 107846 (2021).
27. Smeal, R. M., Rabbitt, R., Biran, R. & Tresco, P. A. Substrate curvature influences the direction of nerve outgrowth. *Ann. Biomed. Eng.* **33**, 376–382 (2005).
28. Smeal, R. M. & Tresco, P. A. The influence of substrate curvature on neurite outgrowth is cell type dependent. *Exp. Neurol.* **213**, 281–292 (2008).
29. Xu, K. et al. Effect of electrical and electromechanical stimulation on PC12 cell proliferation and axon outgrowth. *Front. Bioeng. Biotechnol.* **9**, 757906 (2021).
30. Neudorfer, C. et al. Kilohertz-frequency stimulation of the nervous system: a review of underlying mechanisms. *Brain Stimul.* **14**, 513–530 (2021).
31. Fujita, K., Lazarovici, P. & Guroff, G. Regulation of the differentiation of PC12 pheochromocytoma cells. *Environ. Health Perspect.* **80**, 127–142 (1989).
32. Szeberényi, J. & Erhardt, P. Cellular components of nerve growth factor signaling. *Biochim. Biophys. Acta BBA - Mol. Cell Res.* **1222**, 187–202 (1994).
33. Pollock, J., Krempin, M. & Rudy, B. Differential effects of NGF, FGF, EGF, cAMP, and dexamethasone on neurite outgrowth and sodium channel expression in PC12 cells. *J. Neurosci.* **10**, 2626–2637 (1990).
34. Brill, N. A. & Tyler, D. J. Quantification of human upper extremity nerves and fascicular anatomy. *Muscle Nerve* **56**, 463–471 (2017).
35. Im, J.-H. et al. Evaluation of anatomical and histological characteristics of human peripheral nerves: as an effort to develop an efficient allogeneic nerve graft. *Cell Tissue Bank* **23**, 591–606 (2022).
36. Alexeev, D., Goedecke, N., Snedeker, J. & Ferguson, S. Mechanical evaluation of electrospun poly(ε-caprolactone) single fibers. *Mater. Today Commun.* **24**, 101211 (2020).
37. Eshraghi, S. & Das, S. Mechanical and microstructural properties of polycaprolactone scaffolds with 1-D, 2-D, and 3-D orthogonally oriented porous architectures produced by selective laser sintering. *Acta Biomater.* **6**, 2467–2476 (2010).
38. Schneider, C. A., Rasband, W. S. & Eliceiri, K. W. NIH Image to ImageJ: 25 years of image analysis. *Nat. Methods* **9**, 671–675 (2012).
39. Meijering, E. et al. Design and validation of a tool for neurite tracing and analysis in fluorescence microscopy images. *Cytom. Part J. Int. Soc. Anal. Cytol.* **58**, 167–176 (2004).
40. Jing, W. et al. Study of electrical stimulation with different electric-field intensities in the regulation of the differentiation of PC12 cells. *ACS Chem. Neurosci.* **10**, 348–357 (2019).
41. Sherrell, P. C. et al. Maintaining cytocompatibility of biopolymers through a graphene layer for electrical stimulation of nerve cells. *Adv. Funct. Mater.* **24**, 769–776 (2014).
42. Borah, R., Ingavle, G. C., Sandeman, S. R., Kumar, A. & Mikhalovsky, S. Electrically conductive MEH-PPV:PCL electrospun nanofibres for electrical stimulation of rat PC12 pheochromocytoma cells. *Biomater. Sci.* **6**, 2342–2359 (2018).
43. Park, J. S. et al. Electrical pulsed stimulation of surfaces homogeneously coated with gold nanoparticles to induce neurite outgrowth of PC12 cells. *Langmuir* **25**, 451–457 (2009).

ACKNOWLEDGEMENTS

We gratefully acknowledge Carlsberg Foundation (CF19–0300), the Fundamental Research Funds for the Central Universities and the Youth Teacher International Exchange & Growth Program (No. QNXM20220045), ERC starting grant (22736), Lundbeck NIH Brain Initiative grants (R360-2021-650 and R273-2017-179), Danish Research Institute of Translational Neuroscience (19958); PROMEMO (Center of Excellence for Proteins in Memory funded by the Danish National Research Foundation) (DNRF133), and the Israel Science Foundation (No. 2130/19) for the support of the research.

AUTHOR CONTRIBUTIONS

B.N.J. and Y.W. contributed equally to methodology, investigation, validation, formal analysis, and writing original draft; Y.W.: funding acquisition; A.L.F.: methodology, validation; S.N.: supervision, methodology, funding acquisition; M.D.: supervision, methodology; D.S.: supervision, methodology, and funding acquisition; M.C.: conceptualization, methodology, resources, supervision, writing review & editing, and funding acquisition.

COMPETING INTERESTS

The authors declare no competing interests.

ADDITIONAL INFORMATION

Supplementary information The online version contains supplementary material available at https://doi.org/10.1038/s41528-023-00270-3.

Correspondence and requests for materials should be addressed to Menglin Chen.

Reprints and permission information is available at http://www.nature.com/reprints

Publisher's note Springer Nature remains neutral with regard to jurisdictional claims in published maps and institutional affiliations.